

GENERAL ARTICLE

Aberrant Drp1-mediated mitochondrial division presents in humans with variable outcomes

Brittany N. Whitley¹, Christina Lam², Hong Cui³, Katrina Haude³, Renkui Bai³, Luis Escobar⁴, Afifa Hamilton⁴, Lauren Brady⁵, Mark A. Tarnopolsky^{5,6}, Lauren Dingle⁷, Jonathan Picker⁸, Sharyn Lincoln⁸, Laura L. Lackner⁹, Ian A. Glass² and Suzanne Hoppins^{1,*}

¹University of Washington School of Medicine, Department of Biochemistry, Seattle, WA 98195, USA,

²University of Washington School of Medicine, Division of Genetic Medicine, Department of Pediatrics, Seattle, WA 98145, USA, ³GeneDx, 207 Perry Parkway, Gaithersburg, MD, 20877, USA, ⁴Peyton Manning Children's Hospital at St. Vincent, Medical Genetics & Neurodevelopment Center, Indianapolis, IN, USA, ⁵Department of Pediatrics, McMaster University, Hamilton, ON, L8N 3Z5, Canada, ⁶Department of Medicine, McMaster University, Hamilton, ON, L8N 3Z5, Canada, ⁷Department of Pediatrics, University of Texas Southwestern Medical Center, Dallas, TX, 75390, USA, ⁸Boston Children's Hospital, 300 Longwood Ave., Boston, MA 02115, USA and ⁹Department of Molecular Biosciences, Northwestern University, Evanston, IL 60208, USA

*To whom correspondence should be addressed at: University of Washington Department of Biochemistry 1959 NE Pacific Street Health Sciences Building, J383 Seattle, WA 98195, USA. Tel: (206) 616 7565; Fax (206) 685 1792; Email: shoppins@uw.edu

Abstract

Mitochondrial dynamics, including mitochondrial division, fusion and transport, are integral parts of mitochondrial and cellular function. DNM1L encodes dynamin-related protein 1 (Drp1), a member of the dynamin-related protein family that is required for mitochondrial division. Several *de novo* mutations in DNM1L are associated with a range of disease states. Here we report the identification of five patients with pathogenic or likely pathogenic variants of DNM1L, including two novel variants. Interestingly, all of the positions identified in these Drp1 variants are fully conserved among all members of the dynamin-related protein family that are involved in membrane division and organelle division events. This work builds upon and expands the clinical spectrum associated with Drp1 variants in patients and their impact on mitochondrial division in model cells.

Introduction

Mitochondrial function is essential for many cellular processes. In addition to their canonical role in energy production and metabolism, mitochondria also contribute to lipid biosynthesis, iron cluster formation and other cellular pathways including autophagy, inflammasome activation, telomere maintenance

and apoptotic cell death (1,2). Mitochondria exist as a complex and dynamic network that moves, fuses and divides (3,4). These processes are mediated by conserved protein families and are essential for mitochondrial distribution and quality control.

Mitochondrial division requires the coordinated action of several factors. The actin cytoskeleton and endoplasmic

Received: April 11, 2018. Revised: July 6, 2018. Accepted: July 24, 2018

© The Author(s) 2018. Published by Oxford University Press. All rights reserved.
For Permissions, please email: journals.permissions@oup.com

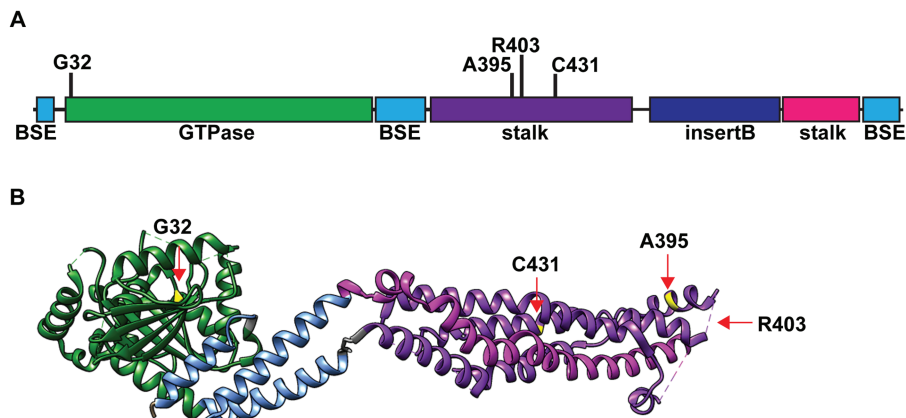


Figure 1. Schematic and structural representation of the position of the mutations identified in this study. (A) Domain structure of Drp1 with mutations reported indicated above. (B) Drp1 structure (PDB 4BE) with position of mutations highlighted in yellow and red arrows. G32 is on a central beta-sheet of the globular GTPase domain. C431 is centrally located in the stalk domain. A395 is toward the bottom of the stalk. While R403 is absent from this structure, the approximate position in a predicted loop is indicated.

reticulum both contribute early in the process of division, cooperating to constrict the diameter of mitochondria (5,6). Further constriction of mitochondria is driven by dynamin-related protein 1 (Drp1), a mechanochemical enzyme encoded by the DNM1L gene (7). The protein is found in the cytosol and is recruited to mitochondria by protein receptors embedded in the mitochondrial outer membrane. There are several different receptors including Mff, Fis1, MiD49 and MiD51 (5). The functional role of each receptor is not clear, but there is evidence to suggest that they can work both cooperatively and independently (8–11). Drp1 assembly is mediated by the stalk domain, which forms a helical bundle that extends from the globular GTPase domain and has multiple interaction surfaces (Fig. 1) (12,13). In the cytosol, Drp1 is a dimer and recruitment to mitochondria by receptors stimulates higher-order assembly of Drp1. Following assembly of a Drp1 ring or helix on the mitochondrial surface, guanosine triphosphate (GTP) binding and hydrolysis drive conformational changes that are coupled to constriction and disassembly (14,15). The final step of mitochondrial division in vertebrates requires a related enzyme, dynamin-2, which works by a mechanism similar to Drp1 and constricts the mitochondria to the very narrow diameter required for separation of membranes (16). Interestingly, many components of the mitochondrial division machine have also been shown to be required for division of peroxisomes (17,18).

Perturbations in mitochondrial division affect cell and organism health. Impaired mitochondrial fusion results in fragmentation of the mitochondrial network, due to ongoing division (19). In contrast, loss of division results in unopposed fusion, causing excessive extension of tubules and interconnection of the network (20). In both cases, mitochondrial distribution and function are compromised. Indeed, loss of Drp1 is embryonic lethal in mice and tissue-specific knockout in the cerebellum is catastrophic, resulting in death within one day of birth (21,22).

Several heterozygous *de novo* missense mutations in DNM1L have been reported in humans (MIM #614388 and 610708). All lethal variants reported thus far are found in the stalk domain (23–25). These patients all presented with central nervous system dysgenesis and neurodegeneration manifesting as hypotonia, developmental regression and an abnormal magnetic resonance imaging (MRI) of the brain. Some pathological variants in the stalk domain of Drp1 support life, but present with seizures and developmental delay. For example, a variant

in the stalk domain (G362D) was identified in a patient who presented with global developmental delay at six months of age and refractory epilepsy at one year (26). Another variant within the stalk domain (R403C) was reported in two unrelated individuals who presented with later onset refractory epilepsy, encephalopathy, developmental regression and myoclonus (27). There are also reports of mutations in the GTPase domain that cause autosomal dominant optic atrophy (E2A and A192E) or hypotonia and developmental delay (T115M) (28,29). The dominant inheritance pattern and the molecular characterization of a few mutant variants together suggest that disease variants have limited protein function and also interfere with the function of wild-type Drp1 in heterozygous patients, likely through heterotypic complex formation (27,30).

Here we describe five patients with mutations in DNM1L. We report two novel *de novo* heterozygous missense mutations, one in the stalk that is lethal (C431Y) and one in the GTPase domain (G32A). In addition, two patients were identified with a pathogenic variant that has been previously reported (R403C). Finally, we report a more modest impact for a missense variant at position A395, compatible with survival (A395G), in contrast to the lethal variant that introduces a charge at that position (A395D). We have also performed functional characterization of each variant to gain insight into the pathophysiology of diseases associated with Drp1 variants. Our data suggests that different variants have unique molecular profiles that lead to a variety of disease states.

Results

Clinical phenotypes of individuals with pathogenic variants in DNM1L varied significantly between genotypes

All five individuals presented with hypotonia and developmental delays and/or regression. The degree of cognitive delay varied among individuals. Half of the individuals were documented to have seizures, but only the individual with the G32A variant exhibited significant ocular involvement. Brain MRI abnormalities and biochemical markers including lactate and very long chain fatty acids were variably abnormal (Table 1 and Supplementary Material).

Table 1.

	Patient 1 DNM1L: c.1292 G > Ap.C431Y	Patient 2 DNM1L: c.1207 C > Tp.R403C	Patient 3 DNM1L: c.1207 C > Tp.R403C	Patient 4 DNM1L: c.95 G > Cp.G32A	Patient 5 DNM1L c.1184 C > Gp.A395G
Current age	Deceased at age 10 months	6 years old	7 years old	7 years old	10 years old
Gender	Female	Female	Male	Female	Female
Developmental delay	+	+	+	+	+
Developmental regression	+	+	+	-	-
Seizures	+	+	+	-	-
Microcephaly	-	-	-	+	-
Optic atrophy	-	-	-	+	-
Nystagmus	-	-	-	+	-
Dysmorphic facies	Unknown	+	-	+	+
Muscle tone abnormalities	+	+	+	+	+ in past, appear to have resolved
Ataxia	-	+	-	+	-
Spasticity	-	+	+	-	-
Failure to thrive	+	-	+	+	-
Gastroesophageal reflux	+	-	+	-	+
Elevated lactate	-	-	+	+	-
Elevated very long chain fatty acids	Unknown	-	Unknown	+	-
Abnormal muscle biopsy	-	+	+	Unknown	Unknown
Abnormal brain MRI	+	+	+	-	+
Abnormal nerve conduction study	Unknown	-	No	+	Unknown
Respiratory chain enzymology results	Data not available	Not performed	Not performed	Skin derived fibroblasts: Normal	Not performed
Other clinical findings	Left hip dysplasia, laryngomalacia, atrial septal defect, central and obstructive sleep apnea, dysphagia, hepatomegaly on exam but ultrasound of abdomen showed normal liver	Dystonia. Muscle derived fibroblasts did not show any deposits or alterations which have been reported in these patients.	Recurrent episodes of supra-refractory status epilepticus, intractable epilepsy, regression, myoclonic movements disorder, tremor, exotropia s/p repair, dysphagia, bilateral ptosis	Progressive scoliosis, short stature, aphthous ulcers,	Hiatal hernia, astigmatism, ADHD, autistic features, hand flapping behaviors

Drp1 G32A patient fibroblast mitochondria are dramatically hyperfused

In fibroblast cells, the mitochondrial network is composed of many tubular organelles distributed throughout the cell. Loss of division activity by deletion or mutation of Drp1 results in dramatic mitochondrial elongation and interconnection due to unopposed mitochondrial fusion (7,21,22). To determine if the novel mutation identified in Patient 4 (G32A) altered mitochon-

drial structure, we visualized mitochondria in patient-derived primary fibroblasts. Indeed, we observed a highly connected mitochondrial network in the patient cells compared to age-matched control fibroblasts (Fig. 2A and B). Many regions of the network formed net-like structures that are characteristic of defective Drp1 function and loss of mitochondrial division (Fig. 2A, inset).

Drp1 has also been implicated in peroxisome division and abundance (31). Peroxisome biosynthesis includes elongation of

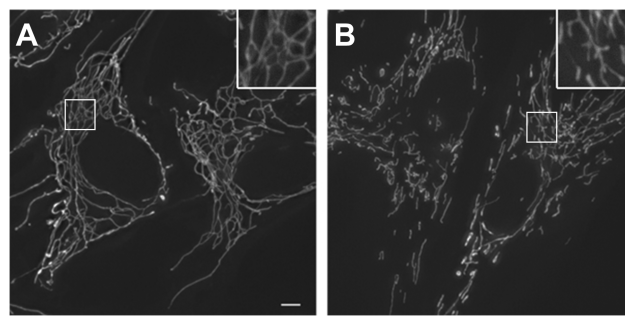


Figure 2. Patient 4 fibroblasts have an extensively connected mitochondrial network. (A) Representative images of primary fibroblasts from Patient 4 (Drp1 G32A). (B) Representative image of primary fibroblasts from an age-matched control. Cells were stained with MitoTracker Red CMXROS and visualized by fluorescence microscopy. Images represent maximum intensity projections. Scale bar 5 μ m.

the organelle, which is followed by Drp1-mediated division. Two reported variants in the stalk of Drp1, G362D and A395D, cause peroxisome elongation in patient fibroblasts, consistent with reduced division activity (23,26). To determine if Drp1-G32A similarly affects peroxisome morphology, we visualized peroxisomes in fibroblasts from Patient 4 and the age-matched control. The observed peroxisome length and number were indistinguishable between control and patient cells, indicating that peroxisome division is not notably altered in the patient fibroblasts (Supplementary Material, Fig. S1).

Drp1 mutant alleles cannot restore normal mitochondrial morphology in Drp1 null cells

To determine how the identified DNM1L mutations affected Drp1-mediated mitochondrial division, we assessed the ability of each mutant to rescue the mitochondrial morphology defect in cells lacking Drp1. HCT116 cells lacking Drp1 ($Drp1^{-/-}$) have an extensively interconnected mitochondrial network (Fig. 3A, empty) (32). Expression of human Drp1 in $Drp1^{-/-}$ cells resulted in the restoration of some shorter mitochondrial tubules (Fig. 3A, wild type (WT)). As controls for Drp1 function, we also included two well-characterized mutants that do not support mitochondrial division, Drp1-K38A and Drp1-G350D, throughout our analysis. Drp1-K38A abolishes GTPase activity by changing a key catalytic residue in the P-loop, which forms the GTP-binding pocket (33). Drp1-G350D is a variant in the stalk domain similar to a previously reported lethal mutation (G350R) and a well-characterized mutation in the yeast division protein, Dnm1 (G385D), which interferes with higher-order self-assembly (24,34,35). As expected, in Drp1 null cells expressing Drp1-K38A or Drp1-G350D, mitochondria remained extensively hyperfused, indicating no Drp1-dependent mitochondrial division (Fig. 3A and B).

Similar to Drp1-K38A, Drp1-G32A changes a conserved residue in the nucleotide-binding domain of Drp1. Mitochondria in $Drp1^{-/-}$ cells expressing Drp1-G32A remained hyperfused, as in Drp1-K38A-expressing cells (Fig. 3A and B). Drp1 $^{-/-}$ cells expressing Drp1-R403C and Drp1-C431Y also showed no rescue, with hyperfused mitochondria in >95% of cells (Fig. 3A and B). Consistent with previously reported data, the Drp1-R403C variant was similarly unable to restore wild-type mitochondria morphology in Drp1-null cells (Fig. 3A and B) (27). Interestingly, ~75% of cells expressing Drp1-A395G had mitochondria with a

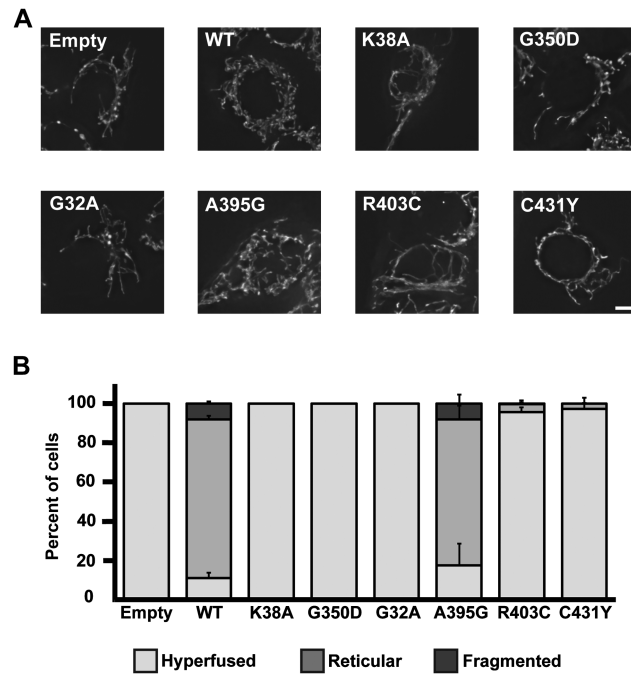


Figure 3. Expression of Drp1 mutants in Drp1 null cells. (A) Representative images of $Drp1^{-/-}$ HCT116 cells transiently expressing Drp1-WT and mutant alleles are shown. Scale bar is 5 μ m. (B) Quantification of mitochondrial morphology in $Drp1^{-/-}$ HCT116 cells expressing Drp1 mutants. Error bars indicate mean + standard deviation from three experiments ($n > 100$ cells per mutant per experiment).

reticular morphology, similar to wild-type cells. This suggests that Drp1-A395G mutant is a hypomorph and can support mitochondrial division when overexpressed.

These variants are at positions that are fully conserved in the members of the dynamin-related protein family that mediate membrane scission events, consistent with critical function. To explore the impact on conserved function, we characterized the variants in Dnm1, the *Saccharomyces cerevisiae* mitochondrial division machine. While Drp1 and Dnm1 are very similar, Drp1 cannot restore division in yeast, consistent with unique mechanisms in each organism (11). To determine if the *de novo* patient mutations alter a fundamental and conserved property intrinsic to the division activity of Drp1 and separate from its regulation or interaction with other proteins, we made the analogous mutations in yeast *dnm1* and expressed these in $\Delta dnm1$ cells to assess Dnm1-mediated mitochondrial division activity. In wild-type yeast, mitochondria are localized to the cell cortex in an extended, branched network (Fig. 4, branched). In contrast, mitochondria in yeast cells lacking Dnm1 form a net-like structure (Fig. 4, hyperfused). Expression of wild-type Dnm1-green fluorescent protein (GFP) resulted in a more branched network compared to $\Delta dnm1$ yeast, consistent with restoration of mitochondrial division. Dnm1-K41A (Drp1 K38A) and Dnm1-G385D (Drp1-G350D) expression in $\Delta dnm1$ yeast did not change the mitochondrial network compared to empty vector controls, consistent with their characterization as non-functional variants (34,36).

As we observed with the human Drp1 mutants, none of the mutations in yeast Dnm1 fully rescued mitochondrial division activity (Fig. 4, Supplementary Material, Fig. S2). Dnm1-G35A (Drp1-G32A) exhibited the most severe phenotype, with virtually no branched networks, consistent with no division activity.

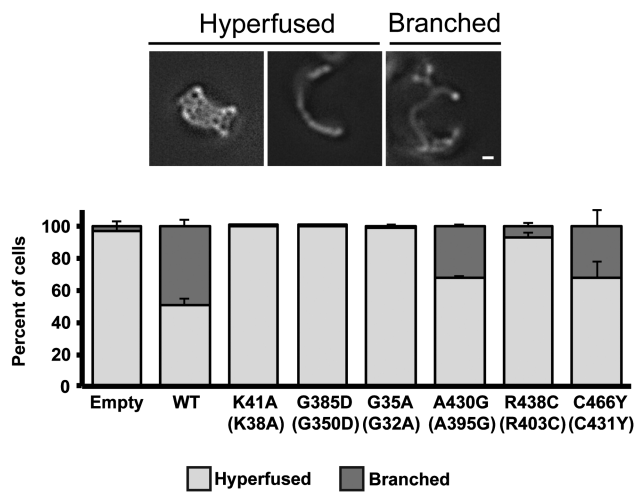


Figure 4. Expression of Dnm1 mutants in Dnm1 null cells to assess division activity. Representative images of different classes of $\Delta dnm1$ yeast are shown. Hyperfused mitochondria include both net and elongated structures (left and middle) while branched mitochondria have more distinguishable tips (right). Scale bar is 1 μm . The graph represents quantification of mitochondrial morphology in $\Delta dnm1$ yeast expressing mitochondrial matrix-targeted dsRed and mutant alleles of Dnm1-GFP. Error bars show mean + standard deviation of three experiments. At least 100 cells counted per mutant in each experiment.

Drp1 stalk domain mutants, Dnm1-A430G (Drp1-A395G) and Dnm1-C466Y (Drp1-C431Y), each showed moderate rescue of division activity in $\Delta dnm1$ yeast, although not as much as wild-type Dnm1. In contrast, cells expressing Dnm1-R438C (Drp1 R403C) had almost no branched mitochondrial networks, indicating that the R403C mutation also disrupts a conserved function of the mitochondrial division machine.

The dominant-negative effects on mitochondrial division by Drp1 variants

Given that the mutations were heterozygous in patients, we set out to assess whether our identified mutant alleles exert a dominant negative effect, which would interfere with the function of the wild-type Drp1. Indeed, the extensive mitochondrial hyperfusion observed in Patient 4 fibroblasts suggests that the G32A allele is dominant-negative (Fig. 2). Previous work indicates that overexpression of Drp1-A395D and Drp1-R403C mutants in wild-type cells inhibits normal division activity (27,30). We expressed Drp1-GFP mutants by transient transfection with a fluorescent mitochondrial matrix marker in wild-type HCT116 cells, which have normal mitochondrial division activity, and scored mitochondrial morphology. We also examined Drp1-GFP assembly and subcellular localization as a proxy for mitochondrial recruitment and higher-order assembly.

Cells expressing the mitochondrial matrix marker alone or wild-type GFP-Drp1 maintained a reticular mitochondrial network and we observed localization of several GFP-Drp1 foci on mitochondria (Fig. 5). Expression of either GFP-Drp1-K38A or GFP-Drp1-G350D resulted in a hyperfused mitochondrial network, as expected for dominant negative mutants (Fig. 5, hyperfused). GFP-Drp1-K38A formed foci on mitochondria while GFP-Drp1-G350D remained completely cytosolic. These data indicate that, while both block activity of the Drp1-WT, these mutations affect different steps in the division pathway, including recruitment to mitochondria and higher-order Drp1 assembly. GFP-Drp1-G32A also had very strong dominant nega-

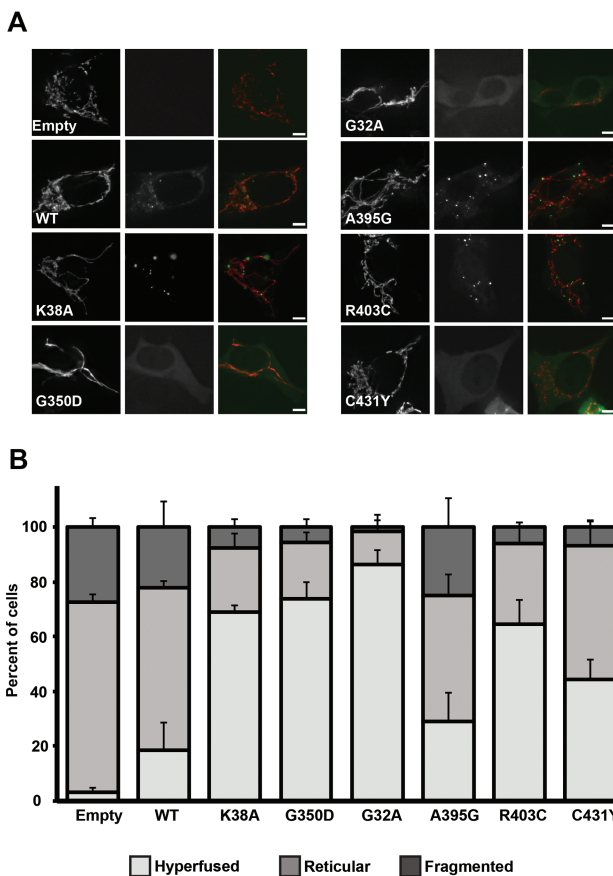


Figure 5. Expression of Drp1 mutants in WT HCT116 cells to assess dominant negative effects. (A) Representative images of wild-type HCT116 cells transiently expressing mitochondrial matrix-dsRed and GFP-Drp1 mutant alleles are shown. The mitochondrial signal (red), GFP-Drp1 (green) and merged signals from a single focal plane are shown. Scale bar is 5 μm . (B) Quantification of mitochondrial morphology in wild-type HCT116 cells. Error bars indicate mean + standard deviation from three experiments ($n > 100$ cells per mutant per experiment).

tive effects, increasing the amount of hyperfused mitochondria from 18.5% in cells expressing Drp1-WT to 86.2% in cells expressing the mutant (Fig. 5A and B). In contrast to GFP-Drp1-K38A, which forms some foci in cells, GFP-Drp1-G32A remained completely cytosolic, and formed no foci on mitochondria. This indicates that GFP-Drp1-G32A has defects in mitochondrial localization and higher-order assembly. GFP-Drp1-A395G and GFP-Drp1-C431Y had a less severe impact on Drp1-WT function, averaging a 1.9-fold increase in the number of cells with hyperfused mitochondria compared to cells expressing GFP-Drp1-WT or the mitochondrial matrix marker alone (Fig. 5A and B). Consistent with this, these mutants show minor defects in mitochondrial recruitment and higher-order assembly in the presence of wild-type Drp1, as all cells expressing these variants show some GFP-Drp1 foci colocalized with mitochondria. Of the stalk domain variants, GFP-Drp1-R403C had stronger dominant negative effects, but GFP-Drp1 recruitment was indistinguishable from the wild-type GFP-Drp1 (Fig. 5A and B).

To determine if the dominant negative properties of these mutants are conserved, we expressed Dnm1 in wild-type (W303) yeast. Mitochondria in wild-type yeast cells expressing Dnm1 are mostly reticular and branched. In contrast, expression of Dnm1-K41A (Drp1-K38A) or Dnm1-G385D (Drp1-G350D) resulted in mitochondria that are highly connected or hyperfused (Fig. 6,

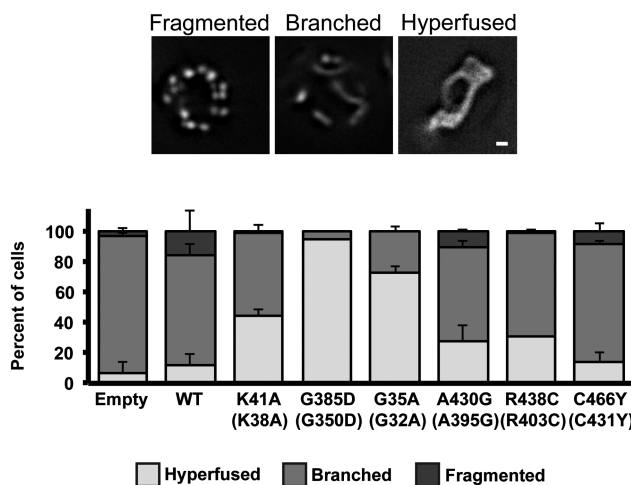


Figure 6. Expression of Dnm1 mutants in wild-type yeast cells to assess dominant negative effects. Representative images of different mitochondrial structures observed in wild-type W303 yeast are shown. Hyperfused mitochondria include both interconnected nets and elongated structures. Scale bar is 1 μ m. The graph represents quantification of mitochondrial morphology in W303 yeast expressing mitochondrial matrix-dsRed and mutant alleles of Dnm1-GFP. Error bars show mean + standard deviation of three experiments ($n > 100$ cells counted in each experiment).

(Supplementary Material, Fig. S3). Once again, Dnm1-G35A (Drp1-G32A) was the most potent dominant negative allele from this group of patient variants, with 75% of cells having hyperfused mitochondria compared to 10% with Dnm1-WT (Fig. 6). In contrast, the stalk domain mutants were only mildly dominant negative, and shifted the population of cells with hyperfused mitochondria from 12% with expression of Dnm1-WT to 15–30% with the mutant proteins (Fig. 6).

Together, these data indicate that all mutant alleles are loss of function, as they cannot fully restore mitochondrial division activity in cells lacking Drp1/Dnm1. Further, Drp1-G32A and Drp1-R403C both demonstrate a robust dominant negative phenotype, indicating that the mutants interfere with the function of the wild-type protein. In these model cells, the A395G and C431Y variants are partially dominant negative by comparison.

Drp1 mutant alleles interact with wild-type Drp1

The dominant negative activity of Drp1/Dnm1 variants suggests that the mutant Drp1 interacts with wild-type Drp1 to inhibit normal division activity. To test this, we assessed direct interactions of the mutants with wild-type Drp1 using a yeast two-hybrid assay. Wild-type Drp1 interacts with itself, as indicated by growth of cells expressing activating domain (AD)-Drp1 and binding domain (BD)-Drp1 (Fig. 7). Drp1-G350D and Drp1-A395D did not interact with Drp1-WT in this assay, consistent with previously published data (30,37). Given the strong inhibition of Drp1 activity in wild-type cells upon expression of these mutants, these data indicate that the yeast two-hybrid does not detect the interaction interface that allows these mutants to assemble with wild-type protein. In contrast, Drp1-K38A and all of the *de novo* mutants described here interact with Drp1-WT, consistent with dominant negative effects.

Discussion

Mitochondria are complex and dynamic organelles, constantly changing their overall structure and organization through the

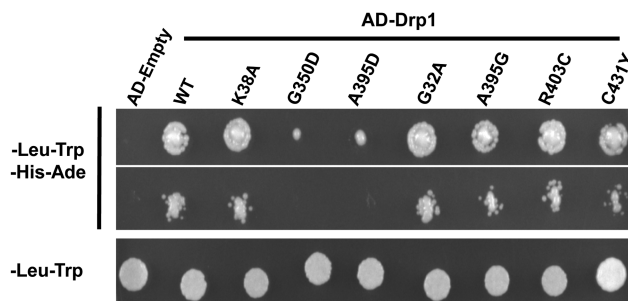


Figure 7. Interaction of Drp1 mutants with wild-type Drp1 by yeast two-hybrid analysis. WT-Drp1 and Drp1 mutants were expressed as GAL4 AD fusions. AD-Drp1 constructs were tested for interaction with wild-type Drp1 expressed as GAL4 DNA BD fusions. Growth at 30°C on adenine and histidine deficient plates indicates protein–protein interaction. The second row represents a 10-fold serial dilution.

coordination of mitochondrial division, fusion and transport. Genetic models that abolish genes encoding proteins required for mitochondrial dynamics illustrate that these activities are required for normal development (21,22). Furthermore, mutations in DNM1L have been reported in patients causing a range of disease states including early lethality, seizures, developmental delay and dominant optic atrophy. Given the spectrum of observed disease outcomes in affected individuals, it is important to fully characterize new disease-associated alleles, to address the dearth in our knowledge of how changes in Drp1 function alter physiology. In this particular condition, this information is of paramount importance for accurate interpretation of DNM1L variants and diagnosis, given the paucity of characteristic and consistent clinical and/or biochemical markers of DNM1L-related disease.

Herein, we report the identification of five patients with pathogenic or likely pathogenic variants mutations in the DNM1L gene, including a novel lethal variant in the stalk domain (C431Y; Patient 1), a previously reported variant (R403C; Patients 2 and 3), a novel missense variant in the GTPase domain (G32A; Patient 4) and a novel missense variant at a previously reported residue (A395G; Patient 5).

All of these variants are of highly conserved amino acids within the dynamin family and were not observed in the general public databases (genome aggregation database (gnomAD), Exome Sequencing Project). *In silico* analysis (Provean, MutTaster, SIFTnew, CADD, PhyloP, PolyPhen-2) predicts that all of these variants are probably damaging to the protein structure/function. To further investigate the functional consequences of these variants, we performed a molecular analysis for their effects upon mitochondrial division in vertebrates and *S. cerevisiae*. The analysis in each model system was internally consistent, indicating that the highly conserved function of the mitochondrial division machine was altered, rather than regulatory pathways or interactions with other proteins. Interestingly, not all alleles exhibit the same strong dominant negative phenotype in the model systems tested here, unlike previously reported disease alleles (27,30). The fact that the variants with partial dominant negative activity do not restore mitochondrial division in cells lacking Drp1 or Dnm1 raises the possibility that the pathophysiology of these diseases includes haploinsufficiency. However, we cannot exclude that the model systems do not fully recapitulate the complexity of human tissues affected in these patients.

Interestingly, our molecular analysis of Drp1-C431Y is discordant with the early death of Patient 1, as the allele is null, but is not the most robust dominant negative activity in the HCT116 and *S. cerevisiae* cells tested here. This suggests that

the defect caused by Drp1-C431Y is minimized in these models but is catastrophic in the context of a specialized cell or tissue type, such as post mitotic neurons. Of significance, this position maps to an assembly interface identified in the crystal structure of Drp1. Other variants in this region (E426A and R430D) were characterized *in vitro* and were indistinguishable from Drp1-WT in their ability to self-assemble, interact with liposomes and hydrolyze GTP (13). In contrast, these mutants did not tubulate liposomes *in vitro*, indicative of a defect in the formation of stable, membrane-anchored assemblies that can constrict mitochondria. While C431 is not implicated in the formation of intramolecular bonds as E426 and E430 are, the mutation to tyrosine could alter the integrity of the interface and impact assembly.

Consistent with previous reports, Patients 2 and 3 (R403C) both presented with seizures and developmental regression. Our functional characterization of Drp1-R403C demonstrates that this mutant cannot support mitochondrial division and is dominant negative (27). Interestingly, this position falls within a highly conserved loop in the dynamin family. One very well characterized mutation in dynamin also falls in this loop and completely abrogates assembly (38).

In both vertebrate cells and in *S. cerevisiae*, Drp1-G32A had the most robust dominant negative phenotype. The complete lack of GFP foci in cells is consistent with an inability to assemble into higher-order structures and there is no apparent recruitment to mitochondria. Patient 4 also presented with optic atrophy. Autosomal dominant optic atrophy was previously reported in patients identified with *de novo* variants in the GTPase domain of Drp1 (28), suggesting that the functional defects associated with variants in this region are distinctly detrimental in this tissue, specifically at the level of ganglion cells. Additionally, this patient was shown to have pure progressive sensory neuropathy, which is likely a major contributor to her ataxia. To our knowledge, pure sensory neuropathy has not been reported previously in DNM1L associated disorders although findings attributable to an underlying neuropathy including ataxia, absent deep tendon reflexes and pain insensitivity have been reported (39). However, sensory neuropathy is well documented in a known mitochondrial fission defect causing Charcot–Marie–Tooth syndrome (40).

The first report of a disease-associated mutation in DNM1L was a lethal variant, Drp1-A395D. This is a dramatic alteration, from a small and neutral amino acid to a large, branched and charged residue. Drp1-A395D was dominant negative in cells and was predicted to disrupt the assembly of Drp1 required for mitochondrial division (30). In contrast, we report a relatively modest change (alanine to glycine) that has a more modest impact on Drp1 function. These data reveal that, while this site is sensitive to changes, the overall impact on Drp1 function can be grossly different dependent on the exact electrophysiological characteristics of the precise amino acid substitution.

Materials and Methods

Research subjects

The guardians of the individuals participating in this study gave written, informed consent through journal publication consents or as part of clinical protocols or waivers approved by the Institutional Review Boards of the respective home institutions. Deoxyribonucleic acid (DNA) was harvested from peripheral whole blood. Fibroblast cultures were established from forearm full thickness skin punch biopsies or quadriceps muscle biopsies obtained for diagnostic purposes. Mitochondrial respiratory

chain analysis, when performed, occurred in a clinical laboratory using previously described methods (41,42).

Whole exome sequencing

Clinical whole exome sequencing (WES) testing was performed for all patients and their parents as described (43). A trio-based design was utilized for WES. Genomic DNA from either whole blood or fibroblasts was extracted and isolated from the affected proband and the probands' parents using standard methods. DNA libraries were generated using the SureSelect Human All Exon V4 or Clinical Research Exome kit (Agilent Technologies, Santa Clara, California, USA). Data were mapped to the NCBI hg19/GRCh37 human genome reference sequence and analyzed using GeneDx's XomeAnalyzer, an interface for variant annotation, filtering and viewing. The mean depth coverage for the DNM1L gene was 96x, and 100% of the coding region and the adjacent intronic regions were covered at $\geq 10x$. Variants identified by WES were evaluated and classified according to published guidelines (44). Whole mitochondrial genome sequencing analysis in DNA extracted from whole blood was performed for patients 3–5; mitochondrial DNA sequence was assembled and analyzed relative to the revised Cambridge Reference Sequence and MITOMAP database (<http://www.mitomap.org>) in combination with concurrent matrilineal relative testing. Identified sequence changes of interest were confirmed via Sanger sequencing, and segregation analysis was performed for family members.

Plasmids and Strains

pcDNA3.1 GFP-Drp1-splice variant 3 (SV3) (7) and pHS20 Dnm1-GFP (45) were used to transfect mammalian and yeast cells, respectively. To construct yeast-two-hybrid plasmids, SV3 of human dynamin-like protein (699 amino acids, NCBI NP_005681.2) was inserted into pGBKT7 and pGADT7 plasmids. Drp1 SV3 was PCR amplified (forward primer – 5'-CGCGGAT CCATGGAGGCCTAAATTCTGTC-3' and reverse primer – 5'-ACGGCTCGACTCACCAAAGATGAGTCTCCCGGA-3') and inserted into pGAD-C1 using BamHI/Sall sites. Drp1 SV3 was then excised from pGAD-C1 using EcoRI/SalI sites and inserted into pGBKT7 using EcoRI/SalI sites and pGADT7 using EcoRI/XbaI sites.

Drp1 mutations were introduced by overlapping PCR mutagenesis with Gibson assembly. To generate mutants for yeast transformation, site-directed mutagenesis PCR of pHS20 Dnm1-GFP was followed by yeast-mediated assembly. Specifically, yeast were transformed with PCR products encoding both halves of the target plasmid with overlapping ends and incubated at 30°C for 2 days. To extract the plasmid, yeast were pelleted from liquid cultures and resuspended in 67 mM KH₂PO₄ with 2.5 mM Zymolase and incubated at 37°C for 1 h. DNA was isolated with GeneJet Miniprep Kit and this was transformed into *Escherichia coli* strain DH5alpha. All plasmids were verified by sequencing.

W303 wild-type (*ade2-1; leu2-3; his3-11, 15; trp1-1; ura3-1; can1-100*) and $\Delta dnm1::KANMX6$ yeast (36) were transformed to image mitochondrial morphology. For yeast-two-hybrid analysis, bait and prey constructs were cotransformed into PJ69-4A yeast (MAT α *trp1-901; leu2-3,112; ura3-52; his3-200; gal4Δ; gal80Δ; GAL2-ADE2; LYS2::GAL1-HIS3; met2::GAL7-lacZ*).

Yeast two-hybrid

Drp1-SV3 pGADT7 variants (prey) were cotransformed with WT-Drp1 pGBKT7 (bait) into PJ64-4A yeast. Transformants

were selected on plates lacking leucine and tryptophan. Serial dilutions of yeast were plated on leucine, tryptophan, histidine and adenine deficient plates to assess protein–protein interactions at 30°C for 2 days. Each experiment was repeated three times.

Cell culture

All cells were grown at 37°C with 5% CO₂ and cultured in Dulbecco's Modified Eagle's Medium (Thermo Fisher Scientific) containing 1X Glutamax (Thermo Fisher Scientific) with 10% fetal bovine serum (Seradigm) and 1% penicillin/streptomycin (Thermo Fisher Scientific). Primary human fibroblasts were obtained by skin biopsy. Control fibroblasts were collected from an age-matched, healthy female subject. Wild-type and Drp1-null HCT116 cells were a gift from Richard Youle (32) [National Institute of Health (NIH), Bethesda, Maryland].

Transfection and microscopy

All cells were plated in No 1.5 glass-bottomed dishes (MatTek). Human fibroblasts were incubated with 0.1 µg/mL MitoTracker Red CMXRos for 30 min before imaging, washed and incubated with complete media for at least 30 min prior to imaging. For peroxisome staining, fibroblasts were incubated with 30PPC (parts per cell) of Cell Light Peroxisome-GFP (Life Technologies) for 16 h at 37°C before imaging. Drp1-null HCT116 cells were plated at 5 × 10⁵ cells per well in a 6-well dish. The following day, 3 µg Drp1-GFP was transfected using Lipofectamine 3000, according to manufacturer's instructions. Cells were split into glass-bottomed dish 16–24 h post-transfection. Drp1-null HCT116 cells were stained with 0.1 µg/mL MitoTracker Red CMXRos and imaged 48 h post-transfection at 37°C with 5% CO₂. Cells expressing similar levels of Drp1-GFP protein were chosen to score mitochondrial morphology (GFP pixel intensity between 9000 and 15 000 units). Wild-type HCT116 cells were plated at 4 × 10⁵ cells per dish. The following day, 50 ng mitochondrial matrix targeted dsRed (mitoRed) and 300 ng Drp1-GFP were transfected with Lipofectamine 2000, according to manufacturer's instructions. Wild-type HCT116 were imaged 16–24 h post-transfection at 37°C with 5% CO₂. A Z-series with a step size of 0.3 µm was collected with a Nikon Ti-E widefield microscope with a 63X numerical aperture (NA) 1.4 oil objective (Nikon), a solid-state light source (Spectra X, Lumencor) and a scientific CMOS camera (Zyla 5.5 Megapixel). Each mutant was transfected and imaged on at least three separate occasions (n > 100 cells per experiment).

Single colony yeast transformants were grown overnight at 30°C in synthetic complete media-Leu-Ura + 2% w/v dextrose to mid-log phase. Yeast cells were sonicated (Fisher Sonic Dismembrator Model 100) at setting 1 for 1 s to separate progeny and recovered at least 1 h at 30°C before imaging. Cells were concentrated by centrifugation and mounted on a 3% low melt agarose pad. All yeast cells were imaged at room temperature using 100x/1.2 oil objective with 1.5X magnification. Three independent yeast clones from two separate transformations were imaged.

Image analysis

Images were deconvolved using eight iterations of 3D Landweber or 3D blind deconvolution (Nikon). Deconvolved images were analyzed using Nikon Elements software. Maximum intensity projections were created using ImageJ Software (NIH). Mitochondrial morphology in mammalian cells was scored as follows:

perfused indicates that the entire mitochondrial network was highly connected, with few mitochondrial tips and lacking any mitochondrial fragments (defined as mitochondria less than 2 µm in length); reticular indicates that fewer than 30% of the mitochondria were fragments; fragmented indicates that more than 30% of the mitochondria were less than 2 µm in length.

Yeast mitochondria were categorized as perfused, branched or fragmented as follows: perfused mitochondria included single, elongated tubes and net structures; branched mitochondria indicate a multinodal connected network distributed throughout the cell with >2 mitochondria tips; and fragmented mitochondria were disconnected in short puncta of 0.5 µm or less.

Supplementary Material

Supplementary Material is available at HMG online.

Acknowledgements

We would like to thank the patients and families for permission to publish this work. We thank Marijn Ford for critical discussion of the manuscript. We thank Richard Youle for sharing the Drp1 null cells.

Conflict of Interest statement. Hong Cui, Katrina Haude and Renkui Bai are employees of GeneDx.

Funding

National Institutes of Health (National Institute of General Medical Science (NIGMS) grant R01GM118509 to S.H.); National Science Foundation Graduate Research Fellowship Program (division of graduate education (DGE) 1256082 to B.W.). Any opinions, findings, and conclusions or recommendations expressed in this material are those of the author(s) and do not necessarily reflect the views of the National Science Foundation. Dr Tarnopolsky would like to acknowledge the donation of Warren Lammert, Kathy Corkins and Dan Wright for support of the Neuromuscular and Neurometabolic Clinic and mitochondrial research.

References

- Mills, E.L., Kelly, B. and O'Neill, L.A.J. (2017) Mitochondria are the powerhouses of immunity. *Nat. Immunol.*, **18**, 488–498.
- Kasahara, A. and Scorrano, L. (2014) Mitochondria: from cell death executioners to regulators of cell differentiation. *Trends Cell Biol.*, **24**, 761–770.
- Chen, H., Chomyn, A. and Chan, D.C. (2005) Disruption of fusion results in mitochondrial heterogeneity and dysfunction. *J. Biol. Chem.*, **280**, 26185–26192.
- Chen, H., McCaffery, J.M. and Chan, D.C. (2007) Mitochondrial fusion protects against neurodegeneration in the cerebellum. *Cell*, **130**, 548–562.
- Kraus, F. and Ryan, M.T. (2017) The constriction and scission machineries involved in mitochondrial fission. *J. Cell Sci.*, **130**, 2953–2960.
- Phillips, M.J. and Voeltz, G.K. (2016) Structure and function of ER membrane contact sites with other organelles. *Nat. Rev. Mol. Cell. Biol.*, **17**, 69–82.

7. Smirnova, E., Griparic, L., Shurland, D.L., van der Bliek, A.M. (2001) Dynamin-related protein Drp1 is required for mitochondrial division in mammalian cells. *Mol. Biol. Cell.*, **12**, 2245–2256.
8. Osellame, L.D., Singh, A.P., Stroud, D.A., Palmer, C.S., Stojanovski, D., Ramachandran, R. and Ryan, M.T. (2016) Cooperative and independent roles of the Drp1 adaptors Mff, MiD49 and MiD51 in mitochondrial fission. *J. Cell Sci.*, **129**, 2170–2181.
9. Shen, Q., Yamano, K., Head, B.P., Kawajiri, S., Cheung, J.T., Wang, C., Cho, J.H., Hattori, N., Youle, R.J., van der Bliek, A.M. (2014) Mutations in Fis1 disrupt orderly disposal of defective mitochondria. *Mol. Biol. Cell.*, **25**, 145–159.
10. Yu, R., Liu, T., Jin, S.B., Ning, C., Lendahl, U., Nistér, M. and Zhao, J. (2017) MIEF1/2 function as adaptors to recruit Drp1 to mitochondria and regulate the association of Drp1 with Mff. *Sci. Rep.*, **7**, 880.
11. Koirala, S., Guo, Q., Kalia, R., Bui, H.T., Eckert, D.M., Frost, A. and Shaw, J.M. (2013) Interchangeable adaptors regulate mitochondrial dynamin assembly for membrane scission. *Proc. Natl. Acad. Sci. U.S.A.*, **110**, E1342–E1351.
12. Antony, B., Burd, C., De Camilli, P., Chen, E., Daumke, O., Faelber, K., Ford, M., Frolov, V.A., Frost, A., Hinshaw, J.E. et al. (2016) Membrane fission by dynamin: what we know and what we need to know. *EMBO J.*, **35**, 2270–2284.
13. Fröhlich, C., Grabiger, S., Schwefel, D., Faelber, K., Rosenbaum, E., Mears, J., Rocks, O. and Daumke, O. (2013) Structural insights into oligomerization and mitochondrial remodelling of dynamin 1-like protein. *EMBO J.*, **32**, 1280–1292.
14. Franey, C.A., Clinton, R.W., Fröhlich, C., Murphy, C. and Mears, J.A. (2017) Cryo-EM studies of Drp1 reveal cardiolipin interactions that activate the helical oligomer. *Sci. Rep.*, **7**, 10744.
15. Mears, J.A., Lackner, L.L., Fang, S., Ingberman, E., Nunnari, J. and Hinshaw, J.E. (2011) Conformational changes in Dnm1 support a contractile mechanism for mitochondrial fission. *Nat. Struct. Mol. Biol.*, **18**, 20–26.
16. Lee, J.E., Westrate, L.M., Wu, H., Page, C. and Voeltz, G.K. (2016) Multiple dynamin family members collaborate to drive mitochondrial division. *Nature*, **540**, 139–143.
17. Schrader, M., Costello, J.L., Godinho, L.F., Azadi, A.S. and Islinger, M. (2016) Proliferation and fission of peroxisomes—An update. *Biochim. Biophys. Acta*, **1863**, 971–983.
18. Mohanty, A. and McBride, H.M. (2013) Emerging roles of mitochondria in the evolution, biogenesis, and function of peroxisomes. *Front. Physiol.*, **4**, 268.
19. Schrepfer, E. and Scorrano, L. (2016) Mitofusins, from mitochondria to metabolism. *Mol. Cell*, **61**, 683–694.
20. Mishra, P. and Chan, D.C. (2014) Mitochondrial dynamics and inheritance during cell division, development and disease. *Nat. Rev. Mol. Cell. Biol.*, **15**, 634–646.
21. Ishihara, N., Nomura, M., Jofuku, A., Kato, H., Suzuki, S.O., Masuda, K., Otera, H., Nakanishi, Y., Nonaka, I., Goto, Y. et al. (2009) Mitochondrial fission factor Drp1 is essential for embryonic development and synapse formation in mice. *Nat. Cell Biol.*, **11**, 958–966.
22. Wakabayashi, J., Zhang, Z., Wakabayashi, N., Tamura, Y., Fukaya, M., Kensler, T.W., Iijima, M. and Sesaki, H. (2009) The dynamin-related GTPase Drp1 is required for embryonic and brain development in mice. *J. Cell Biol.*, **186**, 805–816.
23. Waterham, H.R., Koster, J., van Roermund, C.W., Mooyer, P.A., Wanders, R.J., Leonard, J.V. (2007) A lethal defect of mitochondrial and peroxisomal fission. *N. Engl. J. Med.*, **356**, 1736–1741.
24. Chao, Y.H., Robak, L.A., Xia, F., Koenig, M.K., Adesina, A., Bacino, C.A., Scaglia, F., Bellen, H.J. and Wangler, M.F. (2016) Missense variants in the middle domain of DNM1L in cases of infantile encephalopathy alter peroxisomes and mitochondria when assayed in Drosophila. *Hum. Mol. Genet.*, **25**, 1846–1856.
25. Zaha, K., Matsumoto, H., Itoh, M., Saitsu, H., Kato, K., Kato, M., Ogata, S., Murayama, K., Kishita, Y., Mizuno, Y. et al. (2016) DNM1L-related encephalopathy in infancy with Leigh syndrome-like phenotype and suppression-burst. *Clin. Genet.*, **90**, 472–474.
26. Vanstone, J.R., Smith, A.M., McBride, S., Naas, T., Holcik, M., Antoun, G., Harper, M.E., Michaud, J., Sell, E., Chakraborty, P. et al. (2016) DNM1L-related mitochondrial fission defect presenting as refractory epilepsy. *Eur. J. Hum. Genet.*, **24**, 1084–1088.
27. Fahrner, J.A., Liu, R., Perry, M.S., Klein, J. and Chan, D.C. (2016) A novel de novo dominant negative mutation in DNM1L impairs mitochondrial fission and presents as childhood epileptic encephalopathy. *Am. J. Med. Genet. A*, **170**, 2002–2011.
28. Gerber, S., Charif, M., Chevrollier, A., Chaumette, T., Angebault, C., Kane, M.S., Paris, A., Alban, J., Quiles, M., Delettre, C. et al. (2017) Mutations in DNM1L, as in OPA1, result in dominantly optic atrophy despite opposite effects on mitochondrial fusion and fission. *Brain*, **140**, 2586–2596.
29. Hogarth, K.A., Costford, S.R., Yoon, G., Sondheimer, N. and Maynes, J.T. (2017) DNM1L variant alters baseline mitochondrial function and response to stress in a patient with severe neurological dysfunction. *Biochem. Genet.*, **56**, 56–77.
30. Chang, C.R., Manlandro, C.M., Arnoult, D., Stadler, J., Posey, A.E., Hill, R.B. and Blackstone, C. (2010) A lethal de novo mutation in the middle domain of the dynamin-related GTPase Drp1 impairs higher order assembly and mitochondrial division. *J. Biol. Chem.*, **285**, 32494–32503.
31. Li, X. and Gould, S.J. (2003) The dynamin-like GTPase DLP1 is essential for peroxisome division and is recruited to peroxisomes in part by PEX11. *J. Biol. Chem.*, **278**, 17012–17020.
32. Burman, J.L., Pickles, S., Wang, C., Sekine, S., Vargas, J.N.S., Zhang, Z., Youle, R.J., Nezich, C.L., Wu, X., Hammer, J.A. and Youle, R.J. (2017) Mitochondrial fission facilitates the selective mitophagy of protein aggregates. *J. Cell Biol.*, **216**, 3231–3247.
33. Zhu, P.P., Patterson, A., Stadler, J., Seeburg, D.P., Sheng, M. and Blackstone, C. (2004) Intra- and intermolecular domain interactions of the C-terminal GTPase effector domain of the multimeric dynamin-like GTPase Drp1. *J. Biol. Chem.*, **279**, 35967–35974.
34. Ingberman, E., Perkins, E.M., Marino, M., Mears, J.A., McCaffery, J.M., Hinshaw, J.E. and Nunnari, J. (2005) Dnm1 forms spirals that are structurally tailored to fit mitochondria. *J. Cell Biol.*, **170**, 1021–1027.
35. Bhar, D., Karren, M.A., Babst, M. and Shaw, J.M. (2006) Dimeric Dnm1-G385D interacts with Mdv1 on mitochondria and can be stimulated to assemble into fission complexes containing Mdv1 and Fis1. *J. Biol. Chem.*, **281**, 17312–17320.
36. Naylor, K., Ingberman, E., Okreglak, V., Marino, M., Hinshaw, J.E. and Nunnari, J. (2006) Mdv1 interacts with assembled dnm1 to promote mitochondrial division. *J. Biol. Chem.*, **281**, 2177–2183.
37. Zhu, P.P., Patterson, A., Stadler, J., Seeburg, D.P., Sheng, M. and Blackstone, C. (2004) Intra- and intermolecular domain interactions of the C-terminal GTPase effector domain of the multimeric dynamin-like GTPase Drp1. *J. Biol. Chem.*, **279**, 35967–35974.

38. Ford, M.G., Jenni, S. and Nunnari, J. (2011) The crystal structure of dynamin. *Nature*, **477**, 561–566.
39. Sheffer, R., Douiev, L., Edvardson, S., Shaag, A., Tamimi, K., Soiferman, D., Meiner, V. and Saada, A. (2016) Postnatal microcephaly and pain insensitivity due to a de novo heterozygous DNM1L mutation causing impaired mitochondrial fission and function. *Am. J. Med. Genet. A*, **170**, 1603–1607.
40. Huber, N., Guimaraes, S., Schrader, M., Suter, U. and Niemann, A. (2013) Charcot-Marie-Tooth disease-associated mutants of GDAP1 dissociate its roles in peroxisomal and mitochondrial fission. *EMBO Rep.*, **14**, 545–552.
41. Trounce, I.A., Kim, Y.L., Jun, A.S. and Wallace, D.C. (1996) Assessment of mitochondrial oxidative phosphorylation in patient muscle biopsies, lymphoblasts, and transmitchondrial cell lines. *Methods Enzymol.*, **264**, 484–509.
42. Kirby, D.M., Thorburn, D.R., Turnbull, D.M. and Taylor, R.W. (2007) Biochemical assays of respiratory chain complex activity. *Methods Cell Biol.*, **80**, 93–119.
43. Retterer, K., Juusola, J., Cho, M.T., Vitazka, P., Millan, F., Gibellini, F., Vertino-Bell, A., Smaoui, N., Neidich, J., Monaghan, K.G. et al. (2016) Clinical application of whole-exome sequencing across clinical indications. *Genet. Med.*, **18**, 696–704.
44. Richards, S., Aziz, N., Bale, S., Bick, D., Das, S., Gastier-Foster, J., Grody, W.W., Hegde, M., Lyon, E., Spector, E. et al. (2015) Standards and guidelines for the interpretation of sequence variants: a joint consensus recommendation of the American College of Medical Genetics and Genomics and the Association for Molecular Pathology. *Genet. Med.*, **17**, 405–424.
45. Sesaki, H. and Jensen, R.E. (1999) Division versus fusion: Dnm1p and Fzo1p antagonistically regulate mitochondrial shape. *J. Cell Biol.*, **147**, 699–706.